Visualizing micro leakage position by dynamic measurement in operando hydrogen microscope

Akiko N. Itakura[a*] , Naoya Miyauchi[a], Masahiro Kitajima[a], Taro Yakabe[a], Hajime Yoshida[b]

a National Institute for Materials Science, 1-2-1 Sengen, Tsukuba, Ibaraki 305-0047, Japan

[b] National Institute of Advanced Industrial Science and Technology, 1-1-1 Umezono, Tsukuba, Ibaraki 305-8568, Japan

*corresponding author: itakura.akiko@nims.go.jp

Abstract: We developed an operando hydrogen microscope (OHM) to determine where in materials hydrogen is trapped and causes embrittlement, and the location of hydrogen leak from gas lines, by hydrogen visualization. In the OHM, hydrogen atoms that permeate through a sample are ionized by incident electrons on the sample surface, desorbed into an ultra-high vacuum environment, and then detected. We visualized the surface hydrogen distribution from the hydrogen desorption position. It is also possible to visualize atoms adsorbed from gas phase, as well as gases that leak rather than permeate. The probability that a gas will be adsorbed depends on the substance. The amount of adsorbate increases at a site of locally high pressure. We created guidelines for background evaluation and quantitative analysis of leakage amount under the experimental conditions. Therefore, by visualizing the distribution of adsorbed substances using OHM, we can identify the location of a leak. We visualized a controlled leak of hydrogen in a sintered stainless steel body.

Key words: leaking position; permeation; hydrogen visualization

1. Introduction

We measure hydrogen dynamics by using an ultra-high vacuum (UHV) “operando hydrogen microscope” (OHM). The main component of residual gas in UHV equipment is hydrogen as a fragment of water molecules. Hydrogen is released from the inner wall of the chamber into the vacuum environment even after the water is removed by baking. Very small atoms such as hydrogen can permeate through metals into the vacuum chamber and cannot be efficiently removed by turbomolecular pumps and ion pumps. Outgassing in vacuum systems can be reduced by new materials and by surface treatment techniques such as inner surface polishing, coating, and surface oxidation treatment [1-4]. Outgassing rate is typically measured in samples with a size of anywhere from mm^2 to m^2, and does not take into account surface irregularities due to geometry, structure, or local oxides and elements, or measure the effects of hydrogen release from there.

With society’s need to become carbon neutral, hydrogen holds great promise as a clean energy source. However, it has drawbacks, such as being easily explosive, and, from the perspective of metallurgy, causing embrittlement in metals. To address the problem of hydrogen leaks from pipelines and tanks, it is necessary both to detect the leaks and to investigate the material itself: Where are the leaks? Where are they likely to occur? Has hydrogen embrittlement occurred?

Visualizing the distribution of hydrogen is important for answering these questions but it is difficult to pinpoint its location. It cannot be detected through the use of Auger electron spectroscopy or x-ray photoelectron spectroscopy, techniques used to measure surface composition. However, it can be detected through the use of hydrogen microprinting technology [5, 6], secondary ion mass spectrometry [7, 8], Kelvin probe force microscopy [9], and 3D atom probes [10, 11]. In addition, we developed a new(novel) method, the operando hydrogen microscope (OHM), which visualizes hydrogen by using an electron-stimulated desorption mechanism [12, 13], as explained in section 2.

The OHM can create images of hydrogen on the surface, and signals can be integrated over time. We have measured the local diffusion coefficients of austenite-dominant and martensite-dominant regions in stainless steel (cold-worked, dual-phase SUS304) from changes in the amounts of hydrogen permeating over time [14, 15]. By using electron backscattering diffraction to determine the martensite/austenite ratio of each region and quantitatively calculating the diffusion coefficient in each region, we were able to create a model of hydrogen diffusion through dual-phase regions [16]. We have also confirmed that a chromium oxide film

coating the surface of SUS316 steel more than halved the release of hydrogen from inside the material, and found hydrogen release from hole-like defects where the chromium oxide was incomplete [17], showing that the outgassing from the coated surfaces was not uniform, but that hydrogen is released from specific locations. In this way, OHM measurements can be used to identify local hydrogen release.

We thought that the OHM could be used to visualize leaks in vacuum environments, such as gas leaks from cracks, weld interfaces, and porous materials. Here, we report the visualization of hydrogen leakage through pores of sintered stainless-steel. A standard conductance element (SCE), which allows an open-type reference leak and is based on a sintered stainless-steel filter, was used as a sample [18]. To see when and where hydrogen exits through the filter, we visualized its release from the surface of the filter by OHM. In addition, we quantitatively determined ESD signals by comparison with the SCE from the relation between the number of ESD ions and that of hydrogen molecules leaking through the SCE.

2. Experiment

2.1. Hydrogen visualization by operando hydrogen microscope (OHM)

An OHM is a special type of scanning electron microscope (SEM) that we developed to visualize hydrogen directly and non-destructively. The device consists of an SEM with a detector for ions desorbed by electron-stimulated desorption (ESD) (Fig. 1) [19, 20]. It uses the electron gun, which is normally used for secondary electron images, as an excitation source for ESD. SEM-like ion images are produced. The ion detection mechanism is the same as the OHM device developed in the past [13]. Ions were collected into a detector by a lens beside the sample and detected by a channel plate (F4655-14, Hamamatsu Photonics K.K). The ESD technique can detect a wide variety of surface ion distributions, in particular, that of hydrogen ions, which cannot be obtained with other methods. Hydrogen gas is continuously supplied from the backside "H_2 supply chamber" into the sample, and quickly desorbs into the UHV environment from the other side, which faces the measurement chamber. The system makes it possible to do the ESD measurement of hydrogen that permeates through the surface, with no time limit. The permeation experiment used a hydrogen supply pressure of 100 Pa and an SCE temperature of 373 K, and the ESD signals were integrated over 7 days from a total of 3025 images.

As the OHM does visualize hydrogen focally, its spatial resolution is determined by the electron source of the original SEM. We built three OHMs with different spatial resolutions

from three types of SEMs with different electron beam sources. The OHM used here (ERA 600FEH2, Elionix Inc.) is a modified field emission electron-gun scanning microscope (ERA 600FE, Elionix Inc.), can visualize the hydrogen release position with a spatial resolution of ≤10 nm. The ERA 600FE detects secondary electrons from up to four directions, and can accurately grasp the topographical shape of the surface, even though it is an electron microscope. The OHM used here has secondary electron detectors in two directions, with which we measured hydrogen images and topographic images of the surface at the same time. In the experiment we used electron energy of 2 keV, and the current of 10 pA.

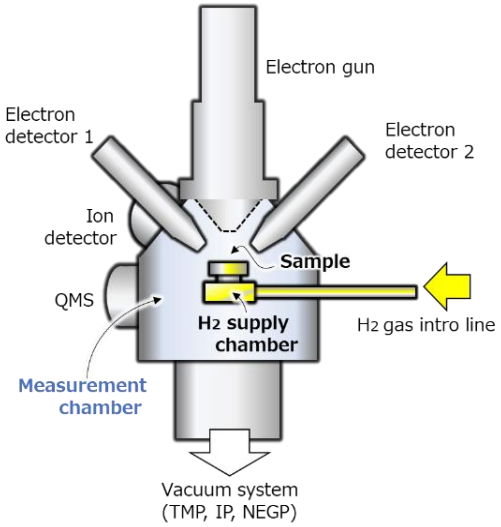

Figure 1. Schematic diagram of high-resolution operando hydrogen microscope (OHM), which uses a field emission (FE) electron gun. TMP, turbomolecular pump; IP, ion pump; NEGP, non-evaporable getter pump; QMS, quadrupole mass spectrometer.

The measurement chamber was evacuated by turbomolecular pump (Edwards Ltd, nEXT300D, 300L/s) and ion pump (Gamma Vacuum, TiTanTV, 240L/s) to 5.70×10^{-8} Pa. The hydrogen supply chamber was evacuated by turbomolecular pump (Pfeiffer Vacuum GmbH, HiPace300, 260 L/s) to 1×10^{-5} Pa. The hydrogen pressure in the supply chamber, P_{H2}, can be controlled between 100 and 2000 Pa. The residual gas in the measurement chamber and the gas molecules passing through the sample were also measured by a quadrupole mass spectrometer (QMS; Pfeiffer, QMG220) using an electron multiplier, and the relation between ESD and QMS signals is discussed. The system is commercially available from Elionix Inc.

2.2. Sample

An SCE (Puaron Japan Co., Ltd.), being a sintered stainless-steel filter used to introduce gas into a vacuum chamber, was used as a sample [18] (Fig. 2). Hydrogen gas was supplied from

below and introduced into the measurement chamber. The electron beam was irradiated at the top of the SCE to obtain the ESD and SEM images before and during hydrogen introduction. The SCE was heated to 373 K by a halogen heater located in the H_2 supply chamber to reduce the adsorption of water molecules to the surface.

The gas molecules pass through the pores of the SCE at the supply pressure of $<10^4$ Pa, because the pore size of the SCE is <1 μm. The molecular flux of H_2 through SCE, Q_{H2}, is calculated as:

$$Q_{H2}(molec./s) = \frac{C_{N2}P_s}{k\sqrt{T \cdot T_0}}\sqrt{\frac{M_{N2}}{M_{H2}}} \quad (1)$$

where C_{N2} is the molecular conductance of SCE for N_2, which was 4.88×10^{-11} m^3/s measured by the manufacturer at T_0 = 298 K; P_s is the hydrogen pressure in the supply chamber, which was raised from 100 to 2000 Pa; k is the Boltzmann constant (= 1.38×10^{-23} J/K); T is the temperature of the supply chamber (= 373 K); and M_{N2} and M_{H2} are the molecular masses of N_2 and H_2, respectively [21].

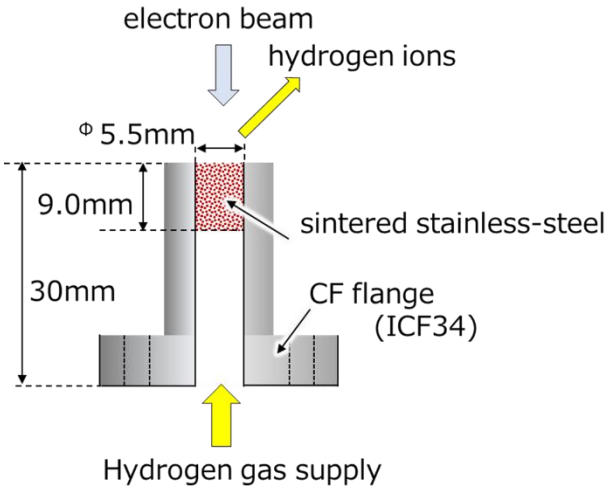

Figure 2. Schematic diagram of standard conductance element (SCE) tested in this study.

3. Results

3.1 Comparison of ESD signal with QMS signal of hydrogen

Figure 3a shows changes in the ESD signal from the surface of the SCE and in the QMS signal of hydrogen (m/z = 2) as the hydrogen supply pressure rises from 100 to 2000 Pa. The QMS signal of hydrogen immediately increased to a constant value, rapidly responding to the step-like rises in the supply of the hydrogen gas to a constant value (ESD signal in Fig. 3a). Such a sudden rise in an ESD signal has not been observed in hydrogen permeation experiments through the bulk, but instead leaked out through numerous pores.

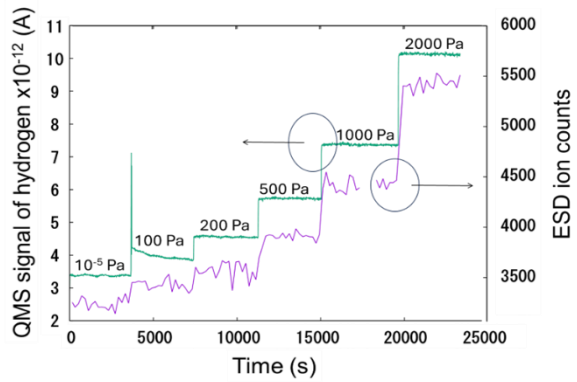

(a)

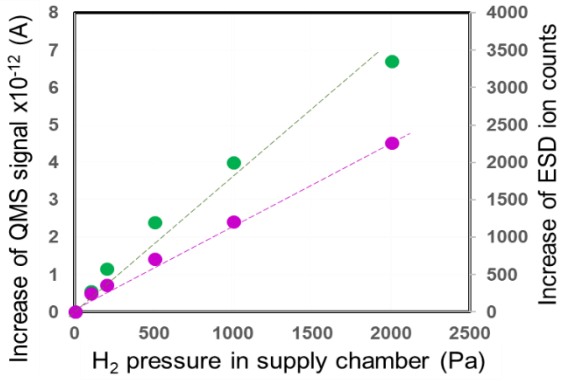

(b)

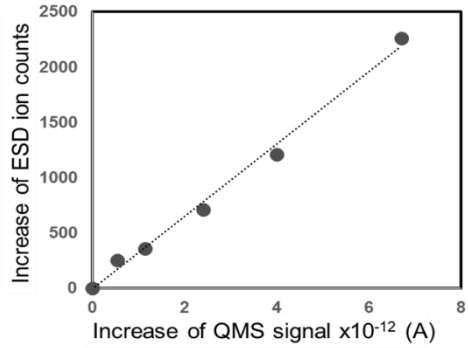

(c)

Figure 3. Relation between QMS and ESD signal. (a) QMS signal of hydrogen (m/z = 2) and ESD ion counts at the same time. Inserted numbers are pressure of hydrogen gas in supply chamber at the time. The background pressure in the supply chamber before hydrogen gas was supplied was 10^{-5} Pa. That in the measurement chamber was 1.54×10^{-7} Pa. The background was not subtracted from the respective signals. The sharp peak in the QMS signal that appeared at 4000 seconds has nothing to do with the essence of the experiment, as it was caused by incorrect operation of the valve that introduced hydrogen into the hydrogen supply chamber. (b) ESD counts and QMS signal in *a*, as a function of pressure in hydrogen supply chamber. To exclude the influence of the background, the values at 10^{-5} Pa in *a* are subtracted from each of the QMS and ESD values. (c) Relation between ESD counts and QMS signal in *a*.

Figure 3c shows the relationship between the ESD ion counts and QMS signals. As the ESD count changes with the width of the measurement area, the linear coefficient is not the same in other sizes of measurement area. The QMS signal is an averaged value corresponding to the number of all hydrogen molecules that passed through the SCE, regardless of the measurement field of SEM view. The value does not change even if the SEM magnification is changed. On the other hand, the ESD ion count is proportional to the number of hydrogen atoms present in the SEM area. When the magnification is increased, the ESD count number differs depending on the local structure, too. For example, it may differ such as when there are many pores in the field of view, even if the field area is the same.

3.2 Background consideration for quantitative measurement

The main residual gas in any UHV environment, such as our measurement chamber, is hydrogen, and the background should not be ignored. The nature of the background varies depending on the target sample, pumps, vacuum equipment material, and test gas. However, it is essential for evaluating the hydrogen passing through the SCE, so we mention it here. We considered individual causes that affect the ESD signal.

Ion signals were observed even when the electron irradiation for ESD measurement was turned off, owing other ion sources: the ion signal in the ESD measurement contains not only hydrogen atoms ionized by electron irradiation on the sample surface, but also residual gas ionized in the ionization chamber of the QMS and residual gas ionized by the ion pump for evacuating the measurement chamber. Ion gauges may also be a source of hydrogen ions. However, we use a cold cathode type ion gauge. There was no increase or decrease in the signal due to turning the ion gauge ON/OFF.

Figure 4a shows the ion counts of ESD when the electron irradiation was turned on and off while the hydrogen pressure in the supply chamber was kept constant at the SCE temperature of 373 K. The number written in the figure as "H_2 leak" is the number of hydrogen molecules leaking through the SCE in the ESD measurement area of 300 μm × 400 μm. The relationship between hydrogen pressure in the supply chamber and ESD counts was measured as the electron irradiation was switched on and off. Figure 4b summarizes it as a function of the number of molecules leaking through the SCE in the ESD measuring area.

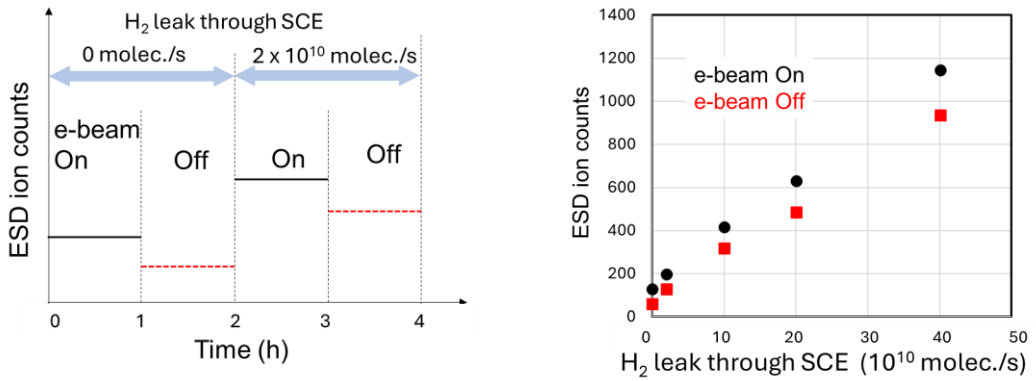

Figure 4. (a) Schematic image of relation between hourly mean ESD ion counts desorbed from the SCE surface and supply pressure in the supply chamber. (b) Ion counts at different supply pressures as electron beam is switched on and off.

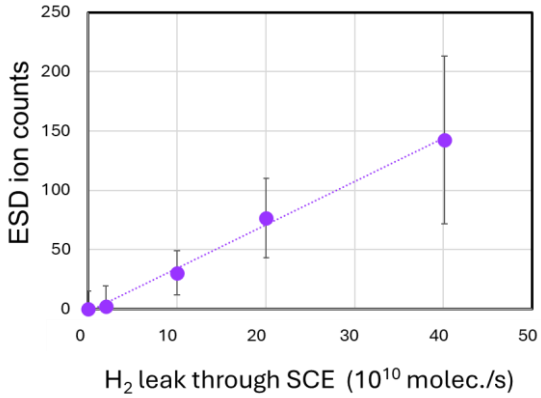

Figure 5. ESD ion counts during desorption from the SCE as a function of hydrogen supply pressure to the backside of the SCE after subtraction of ESD background signals. The SCE temperature was 373 K.

We subtracted the total background (the ion signal when the electron irradiation is off) from the ion signal data. The linear relationship between the ion signal and the amount of hydrogen supplied was maintained (Fig. 5). This relationship shows that one H^+ ion corresponds to 2.67 $\times 10^9$ H_2 molecules (or 5.33 $\times 10^9$ H atoms) in the pressure range.

3.3 Visualize hydrogen passing through SCE

There was a difference in the ESD ion distribution between the part facing the measurement chamber and that nearby the filter pores: hydrogen was highly concentrated on the pore edge area of the particle surface that constitutes the SCE (Fig. 6c). The daily measurements show the distribution of desorbed hydrogen integrated over each 24 h: there was no significant change in

the daily ion distribution (Fig. 7b–h).

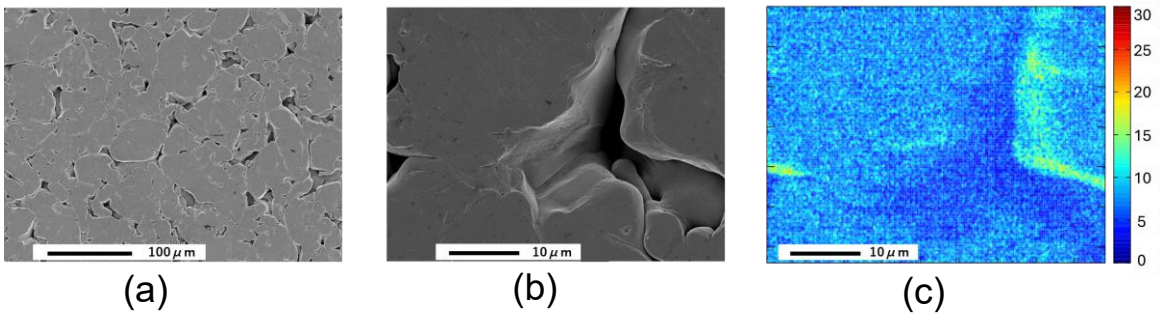

Figure 6. (a, b) SEM images of the surface of the SCE downstream of the hydrogen permeation (a, 300×; b, 2500×); (c) ESD ion image (300 × 225 pixels) of desorption from the same position as in *b*. Sample temperature was 373K, and the ion counts are integrated 7day's data. The color bar shows the ion count from one pixel.

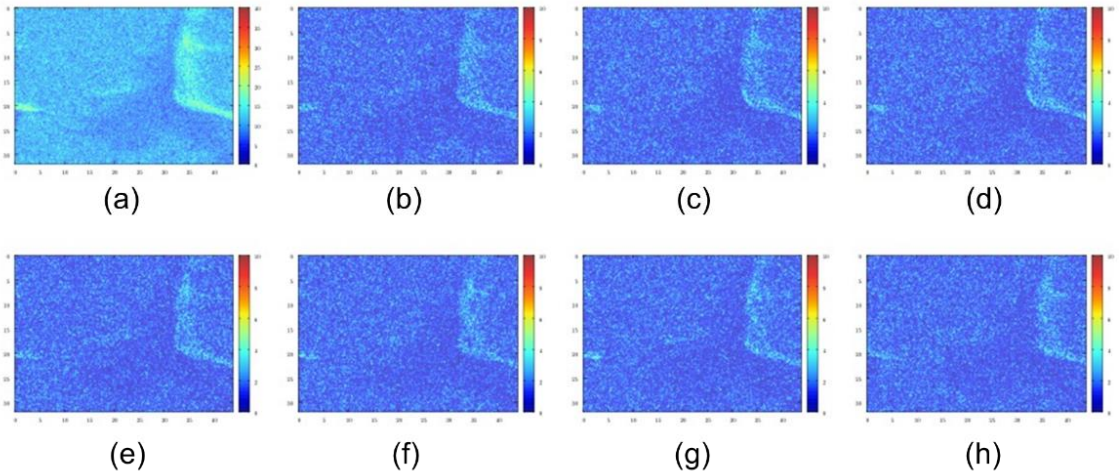

Figure 7. ESD ion images (a) integrated over 1 week; (b–h) daily for 7 days.

4. Discussion

These results show that ESD ion signals come from hydrogen atoms on the metal surface of the SCE. The increase in the ESD ion signal is not due to the hydrogen atoms dissolved within the stainless-steel particles of the SCE or desorbed from the surface. Instead, hydrogen molecules from the hydrogen supply chamber leak through the pores in the SCE and are released into the measurement chamber, increasing the hydrogen pressure there (Fig. 8, Steps 1 and 2). At this time, the pressure difference in the SCE pores between the hydrogen supply chamber and the measurement chamber is 7 to 9 orders of magnitude. Hydrogen molecules in the measurement chamber collide with the surface of the SCE as well as with the inner wall of the chamber, and some are dissociated and adsorbed (Fig. 8; Step 3). The inner walls of the pores and the surface

of the SCE facing the measurement chamber are all made of stainless steel, so hydrogen is adsorbed with the same probability. The local hydrogen pressure in the pores is much higher, then that in the measurement chamber. Therefore, the surface number density of hydrogen atoms is higher near the pores than at the top surface. As a result, ESD signals are greater around a pore.

As shown in Figure 8, we believe that the hydrogen ion signal source comes not only from the atoms that leaked from the pores of the SCE and were adsorbed after being released into the measurement chamber. Another source is the hydrogen atoms dissolved into the stainless-steel particles of SCE. These atoms can diffuse inside the stainless steel and permeate the metal (Fig. 8, "permeate in metal"). However, we consider the influence of these hydrogen atoms on the ESD signal to be negligibly small, because there is no time delay in the ESD signal increase (Fig. 3a); it takes several months for atomic hydrogen diffusion inside metal, as austenite stainless steel, with a thickness of 9.0 mm from the hydrogen supply to the measurement chamber at 373 K[16].

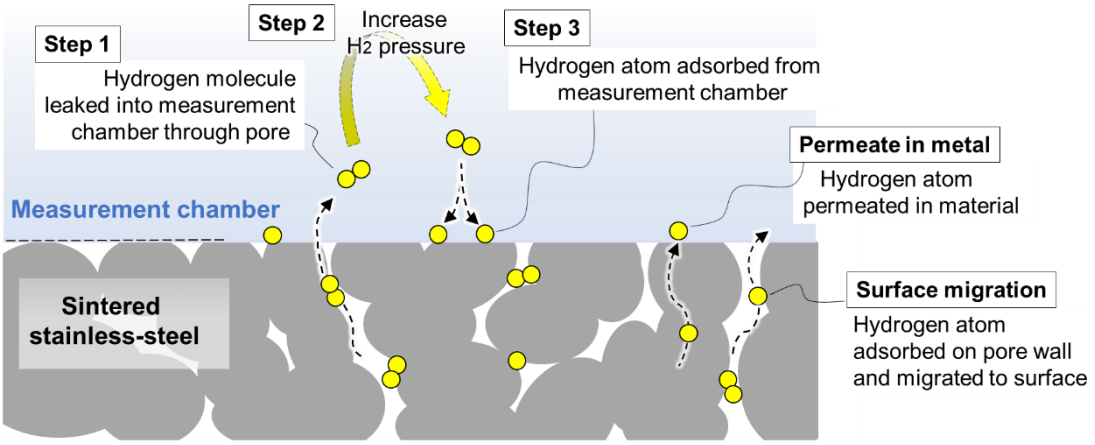

Figure 8. Schematic diagram of hydrogen moving.

Another possible ion signal source is surface migration of hydrogen atoms adsorbed on the pore walls. This hydrogen would be dissociated and adsorbed not only on the surface of the sample after release into the measurement chamber, but also on the inner wall surface of the pores of the leakage route. These atoms might also migrate by surface diffusion to the measurement side surface of the SCE along the surface of the pore walls, at least if they are near the pore exit and the length of diffusion is short.

Let's try to correlate the number of ESD ions with the number of hydrogen molecules passing through the SCE. The flow rate of hydrogen permeating the SCE was calculated based on the data sheet of the SCE obtained from another experiment (see Supplemental S1). The data

sheet shows the conductance when nitrogen gas leaks through the entire SCE, that is, through a 5.5mm diameter opening in the sintered body involved in gas leakage, at a temperature of 298 K (25 degrees), versus the supply pressure (P_s). The molecular flux (Q_{H2}) during the experiment is given by equation (1) [21]. The value is the molecular flux for the entire opening of SCE (S_{SCE}: 2.37 X $10^{-5}m^2$), so the molecular flux (Q_{H2Sm}) from the microscope field of view (S_m) is expressed as follows:

$$Q_{H2Sm} = P_S C_{H2} \frac{S_m}{S_{SCE}} \quad (2)$$

We associate this value with the number of hydrogen ions desorbed from the measurement area. When P_S = 100 Pa and T = 373 K, $Q_{H2} = 4.0 \times 10^{12}$ molec./s. The H_2 molecular flux per ESD measurement area of 300 μm × 400 μm, Q_{H2}, is 2.00×10^{10} molec./s, and per 36 μm × 48 μm is 2.88×10^{8} molec./s. In the ESD measurement in Fig. 7a, on the other hand, the total number of ESD ions was 718 000 in one frame of view of the microscope (36 μm × 48 μm) over 7 days. The flux of ESD ions was 6.87×10^{8} ions/(s·m^2). With the above value of Q_{H2} for the microscope view, the number of hydrogen molecules passing through the SCE per single ESD ion corresponds to 2.43×10^{8} molec./ion. With this information, it is possible to quantitatively determine the number of hydrogen molecules released at a specific point from the number of ESD ions at the other samples.

Of course, these numbers relate to only the current experiment, as the frequency of hydrogen image capturing and the ESD desorption rate vary depending on the material of the sample. In addition, the electron beam is scanned, so there are times and areas where electrons for ESD are not irradiated. The yield of ESD also depends on the SEM magnification, that is, the amount of incident electron current per unit area. However, here we tried to calculate the relationship between the amount of hydrogen molecules permeated and the ESD signal under our specific experimental conditions.

We also roughly estimated the hydrogen pressure near the pore exit. We assume the flat part of the top surface of the SCE facing the measurement chamber to have surface adsorbed hydrogen corresponding to 1.0×10^{-7} Pa in the measurement chamber during the permeation experiment. The ESD ion count in this area was $4.65 \times 10^{14}/m^2$ (Fig. 7). On the other hand, that around the pore was $7.12 \times 10^{14}/m^2$, 1.5× the number on the top surface. From the relationship between hydrogen partial pressure and adsorption amount, we estimated the hydrogen pressure near the pore to be 1.5×10^{-7} Pa.

When a sample has a uniform structure and a uniform element distribution, the permeation rate of hydrogen passing through the sample per unit area would be constant, as

we measured the rate of leakage through the SCE here. If the temperature and the hydrogen supply pressure to the back of the sample are constant, the hydrogen flow rate does not depend on the shape or size of the measurement area. However, the ESD signal of hydrogen may depend on the sizes of the electron beam and the measurement area on account of the balance between the real irradiation area, which comes from the spot diameter of the incident electron beam, and the size of the measurement area. If the measurement area is narrow and the electron beam spot size is large, the electron beam will overlap itself and repeatedly irradiate multiple points on the sample. For this reason, to quantitatively analyze the amount of leakage or permeation, we need to measure the relationship between the amount of gas released and the number of ESD ions in each measurement condition and SEM magnification.

5. Conclusion

Using an operando hydrogen microscope, we imaged hydrogen gas leaking from a sintered body. The hydrogen leaked predominantly from pores. The OHM allowed us to identify very small points where gas leaked. Visualizing the location of local gas leaks from welded metal joints and barrier films to prevent gas diffusion will greatly promote research. However, it is not easy to quantitatively interpret the absolute amount of permeation from the ESD signal, which is the desorbed hydrogen ion count. It is necessary to calibrate the signal and the permeation flux every time the magnification is changed, even with the same material and measurement conditions. By considering the individual effects in detail, it would be possible to relate the signal locally to the molecular flux.

Acknowledgments

We thank Prof. Takagi at Toho University and his students, Mr. Suzuki and Mr. Iwasawa. We also thank Mr. Yuge Masatoyo and Mr. Yasuhiko Kojima, of Elionix Inc., for producing the special OHM and helping us obtain initial data. We further thank Dr. Tomoko Kusawake, and Ms. Kaname Inaishi, of NIMS, for their assistance in data interpretation. This research was supported by a MEXT/JSPS KAKENHI grant (number JP 18H03849).

References

[1] Y. Ishikawa, V. Nemanic, An overview of method to suppress hydrogen outgassing rate from austenitic stainless steel with reference to UHV and XHV, Vacuum 69 (2003) 501-512.
[2] A. Itakura, M. Tosa, S. Ikeda, K. Yoshihara, Hydrogen permeation properties and surface structude of BN-coated stainless steel membrane, Vacuum 47 (1996) 697-700.
[3] S. Tsukahara, S. Inayoshi, Y. Ootsuka, S. Misawa, A. Tanaka, Outgassing Rate and

Morphology of Surface Oxide Layer of Aluminum Alloy for Vacuum Equipment Use, Journal of Vacuum Society Japan 43 (2000) 209-213.
[4] A.N. Itakura, M. Tosa, T. Yakabe, N. Miyauchi, A. Kasahara, T. Miyata, T. Shindo, Low Outgas Surface Treatment of Stainless Steel 316L Using Segregated Chromium Oxide Layer, Vacuum and Surface Science 61 (2018) 675-680.
[5] T.E. Pérez, J. Ovejero-García, Direct observation of hydrogen evolution in the electron microscope scale, Scripta Metallurgica 16 (1982) 161-164.
[6] Y. Momotani, A. Shibata, D. Terada, N. Tsuji, Hydrogen embrittlement behavior at different strain rates in lowcarbon martensitic steel, Materials Today: Proceedings 2S (2015) S735 – S738.
[7] T.Ohtsubo, K.Suzuki, Secondary Ion Mass Spectrometry SIMS IV: Detection of Hydrogen in Steel Using SIMS, Springer, Berlin, Heidelberg, 1984.
[8] V.I. Shvachko, Analysis and investigation of hydrogen in steels by the mass-spectral method, Materials Science 34 (1998) 544-559.
[9] H. Masuda, SKFM observation of SCC on SUS304 stainless steel, Corrosion Science 49 (2007) 120–129.
[10] J. Takahashi, K. Kawakami, T. Tarui, Direct observation of hydrogen-trapping sites in vanadium carbide precipitation steel by atom probe tomography, Scripta Materialia 67 (2012) 213-216.
[11] J.Takahashi, K.Kawakami, Y.Kobayashi, T.Tarui, The first direct observation of hydrogen trapping sites in TiC precipitation-hardening steel through atom probe tomography, Scripta Materialia 63 (2010) 261-264.
[12] N. Miyauchi, K. Hirata, Y. Murase, H.A. Sakaue, T. Yakabe, A.N. Itakura, T. Gotoh, S. Takagi, 2D mapping of hydrogen permeation from a stainless steel membrane, Scripta Materialia 144 (2018) 69-73.
[13] N. Miyauchi, T. Yakabe, Y. Murase, M. Kitajima, S. Takagi, A.N. Itakura, Apparatus design of operando hydrogen microscope for visualization of time-dependent distribution of hydrogen, Journal of Vacuum Science & Technology A 42 (2024) 013201-1-013201-9.
[14] N. Miyauchi, T. Iwasawa, T. Yakabe, M. Tosa, T. Shindo, S. Takagi, A.N. Itakura, Visualization and characterization of localized outgassing position on surface-treated specimens: Chromium oxide layer on stainless steel, Applied Surface Science 492 (2019) 280-284.
[15] T. Iwasawa, N. Miyauchi, S. Takagi, Y. Murase, Y. Yamada, A.N. Itakura, M. Sasaki, Observation of Behavior of Deuterium Permeated Through Stainless Steel, Vacuum and Surface Science 10 (2019) 635–640.
[16] A.N. Itakura, N. Miyauchi, Y. Murase, T. Yakabe, M. Kitajima, S. Aoyagi, Model of local hydrogen permeability in stainless steel with two coexisting structures, Scientific Reports 11 (2021) 8553.
[17] N. Miyauchi, T. Iwasawa, Y. Murase, T. Yakabe, M. Kitajima, S. Takagi, T. Akiyama, S. Aoyagi, A.N. Itakura, Visualization of local hydrogen diffusion in stainless steel using time resolved electron stimulated desorption, Applied Surface Science 527 (2020) 146710(1)-146710(6).
[18] H. Yoshida, K. Arai, H. Akimichi, T. Kobata, Newly developed standard conductance element for in situ calibration of high vacuum gauges, Measurement 45 (2012) 2452-2455.
[19] S. Takagi, T. Goto, Observation of a titanium surface by desorbed ion images with a scanning electron microscope, Surface Science 287/288 (1993) 361-365.
[20] K. Ishikawa, M. Yoshimura, K. Ueda, Y. Sasaki, A new system for two-dimensional analysis of hydrogen on solid surfaces, ReV. Sci. Instrum. 68 (1997) 4103-4106.
[21] H. Yoshida, K. Arai, T. Kobata, In-situ calibration method for ionization gauges and quadrupole mass spectrometers by combining the standard conductance element and the

conductance modulation method (SCE–CM method), Vacuum 101 (2014) 433-439.